Agenzia nazionale per le nuove tecnologie,
l'energia e lo sviluppo economico sostenibile

MINISTERO DELLO SVILUPPO ECONOMICO

Ricerca di Sistema elettrico

Studio preliminare di fattibilità di un tokamak derivato da FAST compatibile con le configurazioni di plasma "Super X"

F. Crisanti, G. Ramogida
G. Di Gironimo, G. Esposito, R. Mozzillo

Report RdS/2013/258

STUDIO PRELIMINARE DI FATTIBILITÀ DI UN TOKAMAK DERIVATO DA FAST COMPATIBILE CON LE CONFIGURAZIONI DI PLASMA “SUPER X”

F. Crisanti, G. Ramogida (ENEA); G. Di Gironimo, G. Esposito . R. Mozzillo, (CREATE)

Settembre 2013

Report Ricerca di Sistema Elettrico

Accordo di Programma Ministero dello Sviluppo Economico - ENEA
Piano Annuale di Realizzazione 2012
Area: Produzione di energia elettrica e protezione dell’ambiente
Progetto: Attività di fisica della fusione complementari a ITER
Obiettivo: D - FAST il nuovo esperimento satellite europeo
Responsabile del Progetto: Ing. Aldo Pizzuto, ENEA

Si ringrazia per la cortese assistenza la Dr.ssa Carla Cristofani e la Dr.ssa Grazia Ginoulhiac, senza il cui impegno l’attività non avrebbe potuto essere completata nella forma e nei tempi previsti.

Contents

Summary

Within the FAST Project, the support obtained by the “Accordo di Programma tra Ministero dello Sviluppo Economico ed ENEA (Obiettivo D: FAST il nuovo esperimento satellite europeo)” has allowed the study of the “Super X” (SX) magnetic topology for the divertor region. Once realized the SX configuration has shown the possibility to decouple the bulk plasma region from the power-exhausting region, however some strong difficulty is emerged when actually trying to implement it on a machine with a standard Aspect Ratio (R/a ≈ 3). The design revision to the plasma chamber and the poloidal field coils system, which have been sketched in a conceptual draw, showed that the increase of the magnetic volume, respect to the plasma volume, is unacceptable because the technological and cost issues are very larger than the benefits on the power exhaust problem. Moreover, these benefits are limited to the outer strike point of the plasma configuration, leaving unresolved the power exhaust problem on the inner side of the machine.

This work, Objective B.3.2.D.2 of the PAR 2012, has been carried out by CREATE with the collaboration and coordination of ENEA. The deliverables expected for the results in this Objective were grouped in this single document, to ease the comprehension of the whole study integrating technology and physics perspectives.

1 Introduction

The conceptual development and design of FAST, a new machine for magnetic fusion experiments proposed as European satellite, is part of the international activities included in the Framework Program accompanying the ITER agreement, besides JT60SA activities. The final objective of this effort is the construction of FAST, a tokamak for fusion experiments with performance intermediate between those of JET (the European tokamak in Culham, England, in operation since 1983) and ITER (the tokamak to be built in Cadarache, France, resulting from an international agreement among the European Union, China, Japan, Russia, India, South Korea and USA). FAST could be operational from the last few years of the construction of ITER, with the aim of preparing the ITER plasma scenarios by simulating the effect of alpha particles by accelerated ions with auxiliary heating systems. This will make it possible to study a burning plasma without the use of tritium. The use of innovative technology for high heat flux components, developed by ENEA, and the capability of running long-lasting plasma pulses will allow the testing of crucial machine components in conditions relevant for the operation of ITER and DEMO (the future demonstration plant for the production of electricity from nuclear fusion). The FAST experiment was designed to be integrated to the JT60SA operations with complementary targets. Consequently, the integration of the experiments on these two machines can ensure an inclusive study of the physics issues still open on the way for DEMO. Moreover, FAST, as a compact and high-performance machine, can provide significant information regarding the possible development of nuclear fusion-fission hybrid reactors able to burn nuclear waste.

The FAST project envisages the construction, possibly in a ENEA site, of a tokamak machine with the related plants for power supply, cooling by cryogenic helium (30 K) and water, plasma heating by mean of radiofrequency (40 MW) and neutral beam injection. It is also included the construction of the diagnostics to measure plasma features, the development of the control system and the construction of proper technologic buildings. FAST was designed to study the plasma under conditions that simulate those of nuclear burning in a reactor, using an innovative and integrated approach to the variation of the parameters characterizing these regimes. FAST can therefore allow significant progress towards the full understanding of the behavior of the plasma and contribute to a more successful exploitation of ITER. These extreme plasma conditions can also provide a proper test bed to validate the advanced technologies for very high heat flux disposal, which will be crucial in the future fusion reactor. ENEA with the Italian industry are currently in the foreground of the development of new technologies able to dispose of the power coming out of the plasma, including solid tungsten mono-blocks and liquid metals (lithium) solutions, actively cooled and able to support high continuous heat loads (up to ~ 20 MW/m^2).

The current FAST design consists in a high magnetic field, high plasma current, compact size (major radius about 1.8 m) tokamak. The machine load assembly comprise 18 coils for the toroidal magnetic field, 6 inner coils for the transformer, 6 outer coils for the poloidal magnetic field, a supporting structure and a toroidal vacuum chamber which includes plasma facing components, among which the divertor. These components must be remotely replaceable due to the nuclear activation of the materials subsequent to the operation of the machine. The coils are made of copper and cooled with gaseous helium at a temperature of 30 K, in order to reduce the electrical resistivity. The coils supporting structure is composed by 18 C-shaped elements, connected between adjacent elements by toroidal structures giving the mechanical coupling. The upper and lower ends of the inner legs of the toroidal field coils are held together by pre-compression rings. The whole load assembly is enclosed in a metallic high-vacuum cryostat to ensure the thermal insulation of the machine. FAST was designed to operate over a wide range of plasma configurations, from those with a high magnetic field and plasma current (toroidal field up to 8.5 T, plasma current up to 10 MA, pulse duration of about 8 s) to those with long lasting plasma (reduced toroidal field up to 3 T, reduced plasma current up to 2 MA, increased pulse duration up to 170 s). The reference configuration provides for a 7.5 T toroidal magnetic field, a 6.5 MA plasma current and a 20 s pulse duration. This large range of

operating parameters involves the need to adopt engineering solutions apt to satisfy different needs in different configurations and in different times of the operation scenario.

In the frame of the Annual Plan of Implementation ("Piano Annuale di Realizzazione") for the year 2012 of the Programme Agreement between the Ministry of Economic Development and ENEA, the activities relating to the Objective D (FAST, the new European satellite experiment) of the Project B.3.2 (Activities of fusion physics complementary to ITER) were focused on the development of new plasma configurations with reduced thermal loads on the plasma-exposed elements for FAST.

This deliverable cover the activities accomplished on the sub-objective D.2 (Activities on the Super-X plasma configuration conceptual study and design of a FAST-like suitable tokamak), addressed to feasibility study of a "Super-X" (SX) magnetic configuration in a tokamak with aspect ratio, size and magnetic field system comparable to FAST. The studies on the SX configuration highlighted its potential advantage in expelling the power coming out of the plasma in a far away region, decoupling thus the characteristics of the plasma core (bulk) from those in the border (edge).

The activities carried out by CREATE and ENEA on this objective with the results achieved are grouped together (to integrate technology and physics perspectives) and reported in the chapters of the next Section 2 as follows:

- d.2.1 Super-X plasma configuration study and design, for a FAST-like tokamak (Chapter 2.1);
- d.2.2 Super-X plasma configuration compatibility with FAST-like magnetic system and plasma chamber, including also the assessment of the design changes necessary to allow this configuration in a FAST-like tokamak (Chapter 2.2);
- d.2.3 Super-X plasma configuration power exhaust and plasma edge-bulk interaction studies (Chapter 2.3).

2 Super-X plasma configuration conceptual study and design of a FAST-like suitable tokamak

The works carried out for the objective D2, described together in the next three chapters to ease the comprehension integrating technology and physics perspectives, allowed the study and design of a plasma equilibrium with Super-X (SX) topology suitable for a FAST-like tokamak. The FAST design was accordingly modified to make it compatible with this SX configuration with a new plasma chamber and a new arrangement and geometry of the Poloidal Field coils. A first assessment of the achieved SX configuration for the purposes of power exhaust analysis and plasma edge-bulk decoupling was also carried out to evaluate possible further optimizations.

This work, Objective B.3.2.D.2 of the PAR 2012, has been carried out by CREATE with the collaboration and coordination of ENEA.

2.1 Super-X plasma configuration study and design (deliverable D2.1)

A steady-state fusion reactor will have much higher heating power P_h and pulse length than ITER , which itself is several times beyond current fusion machines. Invoking the standard measure P_h/R for the severity of the heat flux, we observe the following:

(a) the two largest current tokamaks JET and JT-60 each have $P_h/R \sim 7$,
(b) ITER, with $P_h \sim 120$ MW and $R \sim 6.2$ m, has $P_h/R \sim 20$,
(c) even a moderate fusion reactor [1, 2, 3] ($P_h \sim 400$–720 MW at $R \sim 5$–7 m) will have a much larger $P_h/R \sim 80$–100.

The 2007 ITER Physics Basis identifies divertor limitations as a key roadblock to higher fusion power densities in steady-state scenarios [4]: “The fusion gain in steady state maximizes at low density for constant β_N. The limitation on reducing the density in next generation tokamaks is set by the impact on the divertor”. The super X divertor (SXD) was developed precisely to meet the challenge of high power density simultaneously with lower plasma density. This high power density, coupled with the range of scrape-off layer (SOL) projections, implies that an acceptable divertor operation is, perhaps, the most serious roadblock in the march towards achieving economically desirable power densities for fusion. A high SOL power density leads to operation in the sheath-limited regime — an unacceptable regime associated with high plate erosion, low impurity shielding, low neutral pressures making helium exhaust problematic or virtually impossible, low divertor radiation and high divertor heat fluxes. Attempts to dissipate excess heat via core radiation preclude good confinement, and probably high β [5]. The SXD [6], created via a redesign of the divertor magnetic geometry, appears to offer a simple and robust, axisymmetric solution for high power density divertor operations. By maximizing divertor power capacity, SXD reduces the core radiation burden, and thus enables core plasma operation to attain high density of fusion power production.
The SXD is an improvement upon the X-divertor (XD) [5]. In the XD, flux expansion near the divertor plate was significantly increased by producing an additional X-point near where the separatrix meets the divertor plate. The SXD improves upon this by additionally increasing the major radius of the divertor. This can be done while keeping the main plasma geometry essentially unchanged. Typically, SXD configuration can increase the major radius by a factor of 2–3, and so it is superior to the XD by increasing the wetted area by factors of 2–3, and also similarly increasing the line length. The SXD has the same relative advantage compared with other proposed geometries (placing the divertor plate near the main X-point, extreme plate tilting, snowflake divertor [7], etc.). Compared with previous proposals, the SXD maximizes several advantageous features at once.

The design of a Super-X configuration in a FAST-like tokamak required, first of all, a substantial redesign of the plasma chamber, to make possible the displacement of the divertor plate far from the main X-point. A first attempt to obtain this is showed in Fig. 1, where the new plasma chamber is showed on the right, compared with the FAST one on the left. The Poloidal Field (PF) coils remain substantially unchanged (except for a slight enlargement of the outer coils). In these figures the first wall is unchanged, for reference. This arrangement of the PF coils is obviously fully compatible with the reference Single Null (SN) and Snow Flake (SF) equilibria, showed respectively in Fig. 2 and Fig. 3, but it is not allowing to obtain a satisfactory SXD configuration, due to the need to push away the additional X-point without moving the main X-point. It has been therefore necessary to introduce two new coils, as depicted in Fig. 4. The plasma separatrix and the main features of the Super-X equilibrium are showed in Fig. 5.

Even when implementing these variations (plasma chamber + extra Poloidal Field coils) we can observe that the obtained Super-X (Fig. 5) is marginal compared to the ones showed in Fig. 1 of the Chapter 2.3, with the extra “cost” of having largely increased the magnetic volume, compared to the plasma volume. However from the picture it emerges clearly that our solution “could solve” the problem for the external Strike Point but it would leave unresolved the Power load problem for the internal side. The only solution it would be (probably) to do the machine symmetric, but a choice like this, obviously, would introduce severe technical problems and very large extra costs.

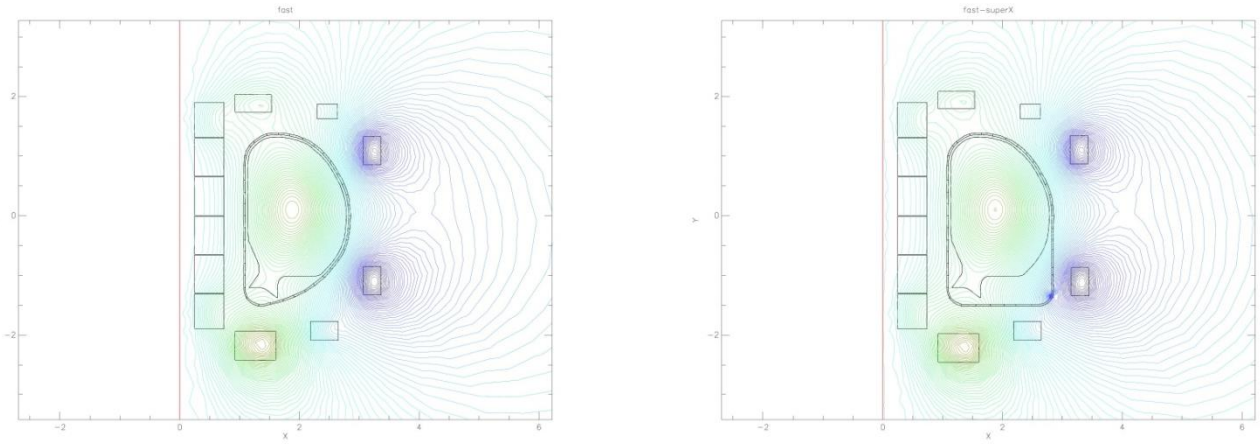

Figure 1. Left: FAST plasma chamber; right: FAST-like Super.X plasma chamber. Isoflux lines for the reference H-mode equilibrium are shown in both the figures.

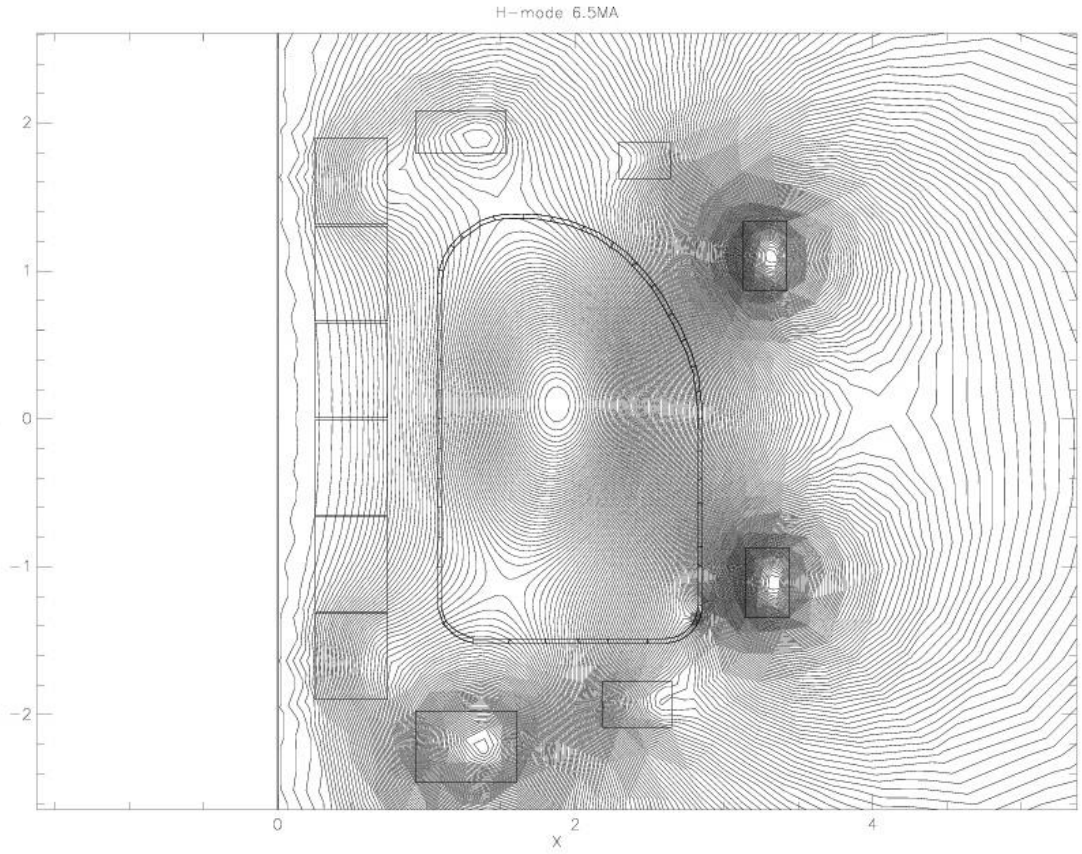

Figure 2. Isoflux contour for the reference H-mode plasma equilibrium in the FAST-like Super-X chamber.

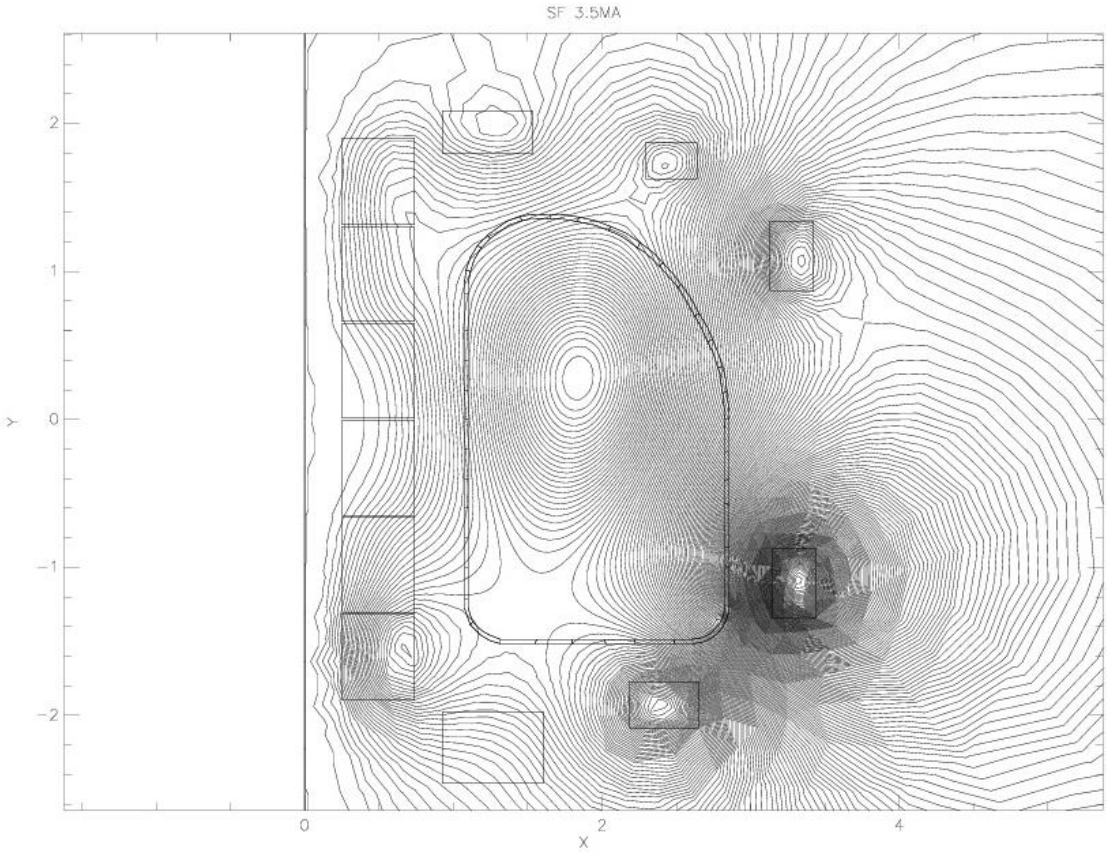

Figure 3. Isoflux contour for the reference Snow Flake plasma equilibrium in the FAST-like Super-X chamber.

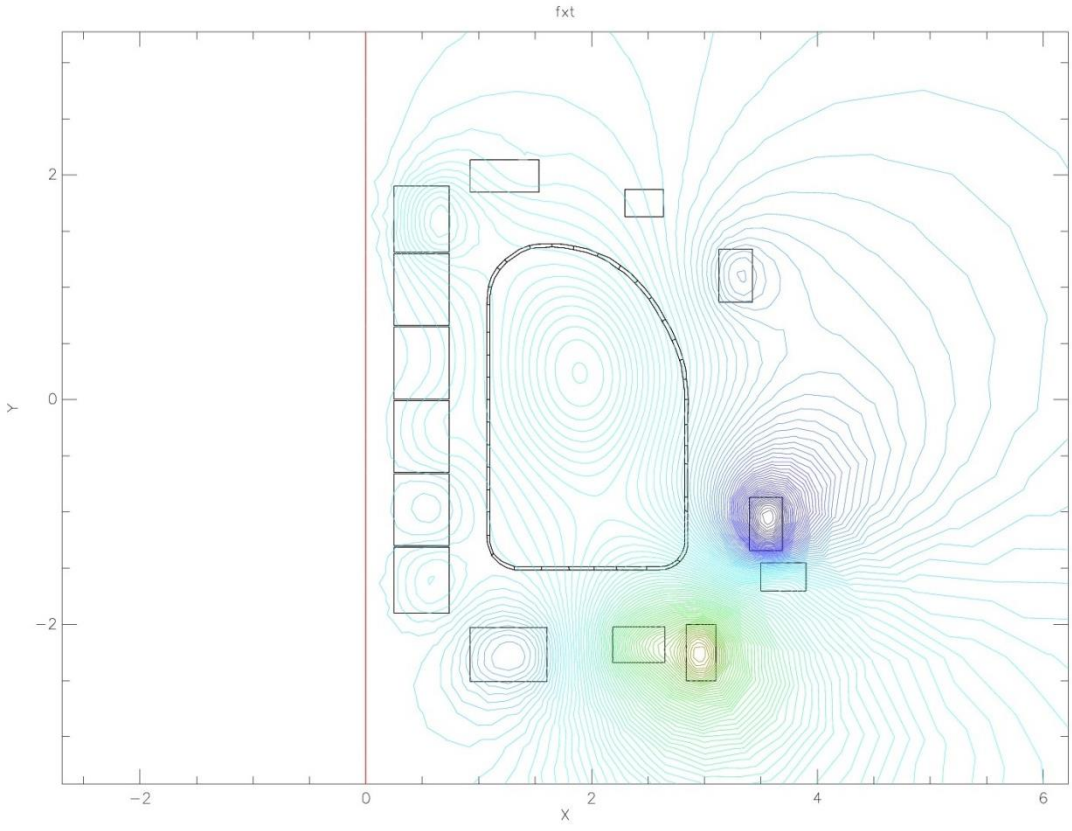

Figure 4. FAST-like Super-X tokamak with the two new coils. Isoflux contour relates to a Super-X equilibrium.

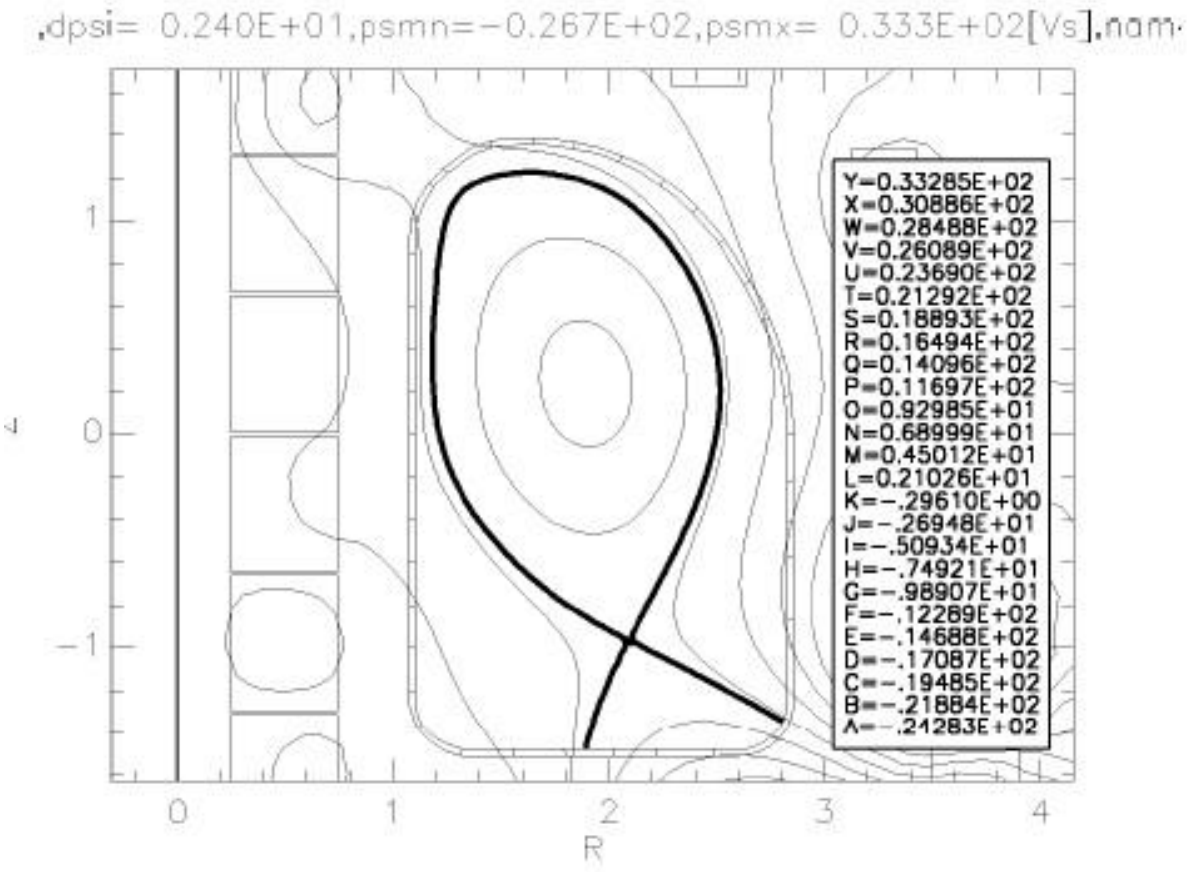

GENERAL DATA

Volume	=0.248E+02	Total Moment	=0.114E+02	Is Second X-	=0.000E+00
LowerTria-95	=0.100E-02	Power-eddy	=0.000E+00	Zeffective	=0.100E+01
UpperTria-95	=0.282E+00	Eddy-low	=0.000E+00	Tau,e,t	=0.474E+00
LowerTriang	=0.100E-02	Eddy-up	=0.000E+00	P,add. heati	=0.000E+00
UpperTriang	=0.310E+00	Atum[eddy]	=0.000E+00	P,ohmic	=0.782E+07
kJb	=0.150E+02	Fz:Halo	=-.176E+04	P,transport	=-.153E+07
kJa	=0.107E+02	Fr:Halo	=0.200E+07	P,alfa	=0.167E+04
Elong-95	=0.154E+01	glonodes	=0.000E+00	P,radiated	=-.951E+05
Elongation	=0.165E+01	FnodeHaloZ	=0.000E+00	Int[p]dv *3/	=0.725E+06
growthtime	=0.857E+02	FnodeHaloR	=0.000E+00	Psb-Ps(Sol)	=0.608E+00
IsLimiter?	=0.000E+00	Ipol@At0	=-.833E+00	Plasma Ohm	=0.241E+11
Z[Xpoint]	=-.961E+00	q[halo midp]	=0.200E+02	Peak FW Jt*B	=0.000E+00
R[Xpoint]	=0.207E+01	Toroidalflux	=0.171E+02	Z Strike 2	=-.149E+01
Z[Halopoint2	=0.000E+00	Poloidalvolt	=0.000E+00	R Strike 2	=0.189E+01
R[Halopoint2	=0.000E+00	Paramag.tflu	=0.669E-01	Z Strike 1	=-.135E+01
Z[Halopoint1	=0.000E+00	Vloop-low	=0.000E+00	R Strike 1	=0.281E+01
R[Halopoint1	=0.000E+00	Vloop-up	=0.000E+00	Halo:20%peak	=0.100E+01
Z[limiter]	=0.000E+00	(psa-psb)	=0.499E+01	Halo:10%peak	=0.100E+01
R[limiter]	=0.000E+00	(psi)av	=0.802E+01	CEjima	=0.000E+00
Rbar	=0.183E+01	Psi-boundary	=0.498E+01	Res.Flattop	=0.000E+00
rminor	=0.666E+00	Psi-axis	=0.996E+01	Psibar q-saw	=0.000E+00
Rmajor	=0.185E+01	J-axis	=0.305E+07	q-sawteeth	=0.000E+00
Zmax	=0.123E+01	Shear95%	=0.377E+01	Helicity	=0.304E+02
Zmin	=-.966E+00	q95formula	=0.612E+01	Energy:poloi	=0.158E+09
Rmax	=0.251E+01	q95	=0.600E+01	Ext-linked f	=-.163E+01
Rmin	=0.118E+01	qaxis	=0.217E+01	Fz:plasma<>c	=0.157E+05
Zaxis	=0.230E+00	qcyl	=0.495E+01	Lp	=0.322E-05
Raxis	=0.188E+01	Betanormal	=0.163E+00	Fz:PS<>circ.	=0.000E+00
VZjcentre	=0.000E+00	Betastar	=0.145E+00	Fz:PS	=0.000E+00
VRjcentre	=0.000E+00	Betafi	=0.100E+00	Fz:Iatal-Fz:	=0.342E+06
Zjcentre	=0.241E+00	p-axis	=0.775E+05	Fz:Iatal	=0.340E+06
Rjcentre	=0.183E+01	betap(1)	=0.116E+00	Circ.Amp	=0.370E+08
R*Btor	=0.135E+02	li(3)	=0.875E+00	Circ.Amp*m	=0.312E+09
Time	=0.000E+00	Surface(sec)	=0.215E+01	Power-circ	=0.000E+00
Iplasma	=0.300E+07	Surface(ext)	=0.638E+02	Atum[circ.]	=0.905E+07

Figure 5. FAST-like Super-X plasma equilibrium separatrix and main features.

2.2 Super-X plasma configuration compatibility with FAST-like magnetic system and plasma chamber (deliverable D2.2)

The Poloidal Field (PF) coil system for a possible FAST-like Super-X tokamak require at least slight changes in the coils radial position and the provision of two additional coil in the lower part of the machine, namely PF4a and PF5a, necessary to create the multipolar field with the additional X-point in the outer low corner of the plasma chamber. This is the smallest essential change: however, to obtain finest plasma equilibria, the need to introduce also more coils will occur. This minimum PF system ensures the capability to obtain Single Null (SN), Snow Flake (SF) and Super-X (SX) equilibria, as shown in Fig. 1 (reference H-mode SN configuration), Fig. 3 (SF) and Fig. 5 (SX). The plasma shape and features are substantially unchanged respect to the reference FAST tokamak, as shown in Fig. 2 (SN) and Fig. 4 (SF). Next figures show the plasma current density for the different equilibria in both current FAST and Super-X FAST: Fig. 6 (SN), Fig. 7 (SF) and Fig. 8 (SX, only in Super-X FAST). It has been used the MHD FEM code Maxfea [1].

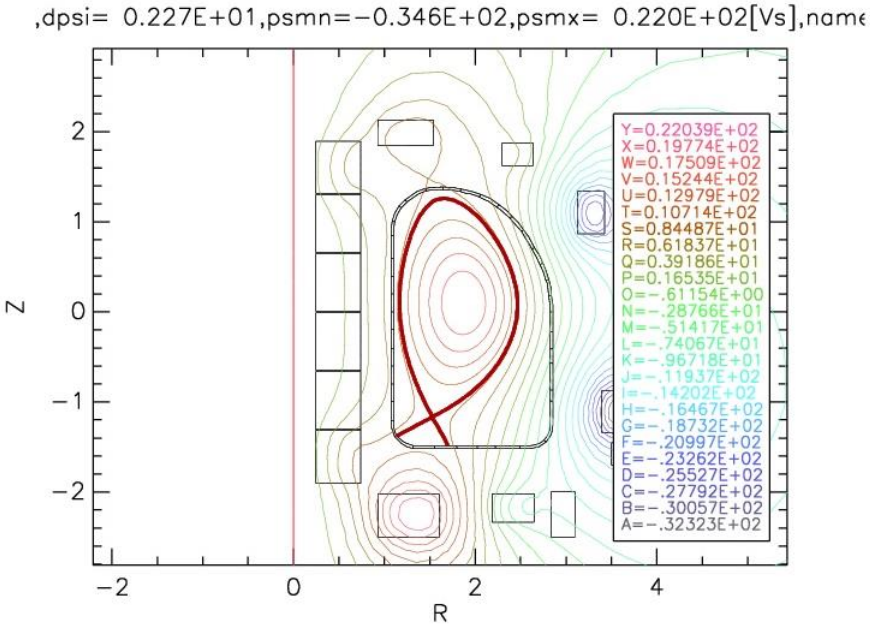

GENERAL DATA

Volume	=0.250E+02	Total Moment	=−.122E+03	Is·Second·X·	=0.000E+00
Lower[ria−95	=0.287E+00	Power−eddy	=0.000E+00	Zeffective	=0.100E+01
Upper[ria−95	=0.211E+00	Eddy−low	=0.000E+00	Tau,e,t	=0.481E+00
Lower[riang	=0.450E+00	Eddy−up	=0.000E+00	P,add., heati	=0.000E+00
Upper[riang	=0.258E+00	Aturn[eddy]	=0.000E+00	P,ohmic	=0.519E+06
kJb	=0.164E+02	Fz:Halo	=−.872E+04	P,transport	=−.250E+08
kJa	=0.105E+02	Fr:Halo	=0.270E+07	P,alfa	=0.000E+00
Elong−95	=0.171E+01	glonodes	=0.000E+00	P,radiated	=−.387E+06
Elongation	=0.186E+01	FnodeHaloZ	=0.000E+00	Int[p]dv •3/	=0.120E+08
growthtime	=0.000E+00	FnodeHaloR	=0.000E+00	Psb−Ps(Sol)	=0.137E+01
Is Limiter?	=0.000E+00	Ipol@Af0	=−.833E+00	Plasma Ohm ∓	=0.995E+11
Z[Xpoint]	=−.116E+01	q[halo midp]	=0.644E+01	Peak FW Jt•B	=0.000E+00
R[Xpoint]	=0.152E+01	Toroidalflux	=0.187E+02	Z Strike 2	=−.138E+01
Z[Halopoint2	=0.000E+00	Poloidalvolt	=0.000E+00	R Strike 2	=0.114E+01
R[Halopoint2	=0.000E+00	Paramag.tflu	=0.206E+00	Z Strike 1	=−.149E+01
Z[Halopoint1	=0.000E+00	Vloop−low	=0.000E+00	R Strike 1	=0.170E+01
R[Halopoint1	=0.000E+00	Vloop−up	=0.000E+00	Halo:20%peak	=0.100E+01
Z[limiter]	=0.000E+00	(psq−psb)	=0.105E+02	Halo:10%peak	=0.100E+01
R[limiter]	=0.000E+00	(psi)av	=0.153E+02	CEjima	=0.000E+00
Rbar	=0.178E+01	Psi−boundary	=0.894E+01	Res.Flattop	=0.000E+00
rminor	=0.649E+00	Psi−axis	=0.194E+02	Psibar q−saw	=0.000E+00
Rmajor	=0.182E+01	J−axis	=0.660E+07	q−sawteeth	=0.000E+00
Zmax	=0.126E+01	Shear95%	=0.490E+01	Helicity	=0.672E+02
Zmin	=−.116E+01	q95formula	=0.346E+01	Energy:poloi	=0.241E+09
Rmax	=0.247E+01	q95	=0.336E+01	Ext·linked f	=−.516E+01
Rmin	=0.117E+01	qaxis	=0.106E+01	Fz:plasma<>c	=0.330E+05
Zaxis	=0.112E+00	qcyl	=0.281E+01	Lp	=0.315E−05
Raxis	=0.188E+01	Betanormal	=0.118E+01	Fz:PS<>circ.	=0.000E+00
VZjcentre	=0.000E+00	Betastar	=0.233E+01	Fz:PS	=0.000E+00
VRjcentre	=0.000E+00	Betafi	=0.159E+01	Fz:Total−Fz:	=0.188E+07
Zjcentre	=0.102E+00	p−axis	=0.130E+07	Fz:Total	=0.187E+07
Rjcentre	=0.181E+01	betap(1)	=0.440E+00	Circ.|Amp|	=0.323E+08
R•Btor	=0.135E+02	li(3)	=0.856E+00	Circ.|Amp|•m	=0.275E+09
Time	=0.000E+00	Surface(sec)	=0.224E+01	Power−circ	=0.000E+00
Iplasma	=0.650E+07	Surface(ext)	=0.639E+02	Aturn[circ.]	=0.147E+08

Figure 1. FAST-like Super-X: reference H-mode Single Null plasma shape and features.

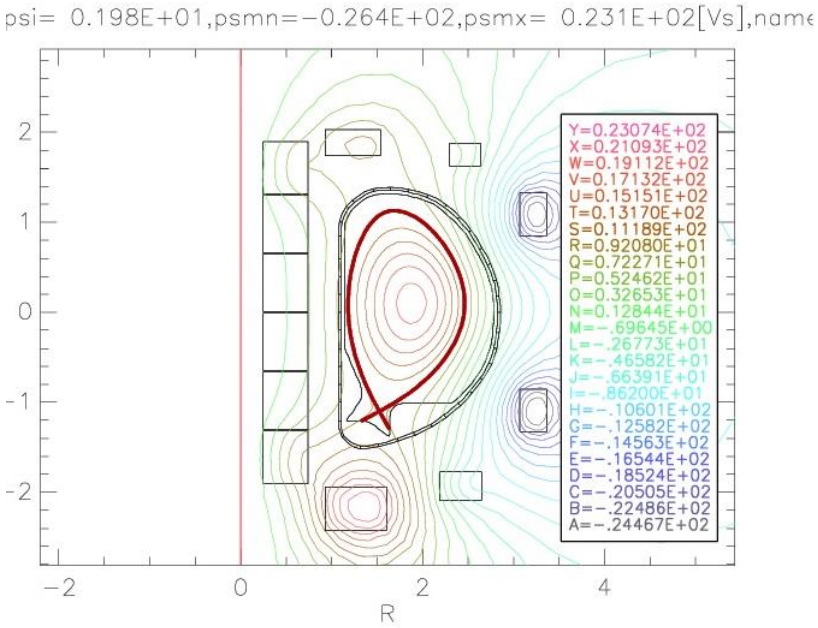

GENERAL DATA

Volume	=0.227E+02	Total Moment	=−.809E+02	Is·Second·X·	=0.000E+00
LowerTria−95	=0.308E+00	Power−eddy	=0.000E+00	Zeffective	=0.100E+01
UpperTria−95	=0.183E+00	Eddy−low	=0.000E+00	Tau,e,t	=0.417E+00
LowerTriang	=0.431E+00	Eddy−up	=0.000E+00	P,add. heati	=0.561E−44
UpperTriang	=0.232E+00	Aturn[eddy]	=0.000E+00	P,ohmic	=0.471E+06
kJb	=0.148E+02	Fz:Halo	=−.920E+02	P,transport	=−.296E+08
kJa	=0.102E+02	Fr:Halo	=0.276E+07	P,alfa	=0.000E+00
Elong−95	=0.160E+01	qlonodes	=0.000E+00	P,radiated	=−.375E+06
Elongation	=0.174E+01	FnodeHaloZ	=0.000E+00	Int[p]dv *3/	=0.123E+08
growthtime	=0.000E+00	FnodeHaloR	=0.000E+00	Psb−Ps(Sol)	=0.138E+01
IsLimiter?	=0.000E+00	Ipol@Af0	=−.833E+00	Plasma Ohm P	=0.103E+12
Z[Xpoint]	=−.109E+01	q[halo midp]	=0.614E+01	Peak FW Jt*B	=0.000E+00
R[Xpoint]	=0.152E+01	Toroidalflux	=0.169E+02	Z Strike 2	=−.121E+01
Z[Halopoint2	=0.000E+00	Poloidalvolt	=0.000E+00	R Strike 2	=0.132E+01
R[Halopoint2	=0.000E+00	Paramag.tflu	=0.211E+00	Z Strike 1	=−.130E+01
Z[Halopoint1	=0.000E+00	Vloop−low	=0.000E+00	R Strike 1	=0.164E+01
R[Halopoint1	=0.000E+00	Vloop−up	=0.000E+00	Halo:20%peak	=0.100E+01
Z[limiter]	=0.000E+00	(psq−psb)	=0.107E+02	Halo:10%peak	=0.100E+01
R[limiter]	=0.000E+00	(psi)av	=0.158E+02	CEjima	=0.000E+00
Rbar	=0.178E+01	Psi−boundary	=0.930E+01	Res.Flattop	=0.000E+00
rminor	=0.641E+00	Psi−axis	=0.200E+02	Psibar q−saw	=0.000E+00
Rmajor	=0.182E+01	J−axis	=0.721E+07	q−sawteeth	=0.000E+00
Zmax	=0.113E+01	Shear95%	=0.453E+01	Helicity	=0.630E+02
Zmin	=−.110E+01	q95formula	=0.302E+01	Energy:poloi	=0.228E+09
Rmax	=0.246E+01	q95	=0.288E+01	Ext·linked f	=−.547E+01
Rmin	=0.118E+01	qaxis	=0.959E+00	Fz:plasma<>c	=0.352E+05
Zaxis	=0.112E+00	qcyl	=0.247E+01	Lp	=0.328E−05
Raxis	=0.188E+01	Betanormal	=0.132E+01	Fz:PS<>circ.	=0.000E+00
VZjcentre	=0.000E+00	Betastar	=0.263E+01	Fz:PS	=0.000E+00
VRjcentre	=0.000E+00	Betafi	=0.181E+01	Fz:Total−Fz:	=0.449E+07
Zjcentre	=0.947E−01	p−axis	=0.146E+07	Fz:Total	=0.449E+07
Rjcentre	=0.181E+01	betap(1)	=0.439E+00	Circ.Amp]	=0.316E+08
R*Btor	=0.135E+02	li(3)	=0.883E+00	Circ.Amp]*m	=0.257E+09
Time	=0.000E+00	Surface(sec)	=0.203E+01	Power−circ	=0.000E+00
Iplasma	=0.650E+07	Surface(ext)	=0.602E+02	Aturn[circ.]	=0.150E+08

Figure 2. Current FAST design: reference H-mode Single Null plasma shape and features.

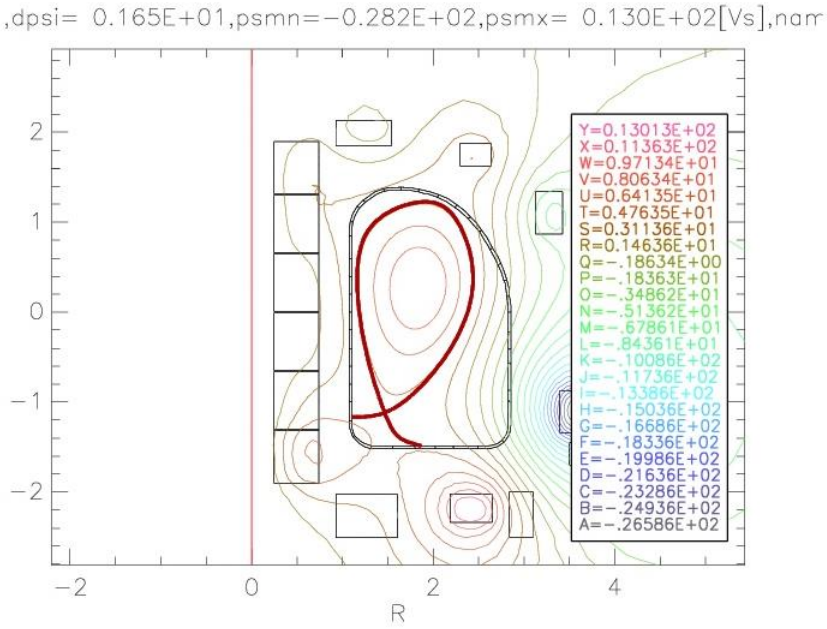

GENERAL DATA

Volume	=0.239E+02	Total Moment	=−.578E+02	Is·Second·X·	=0.000E+00
LowerTria−95	=0.282E+00	Power−eddy	=0.000E+00	Zeffective	=0.100E+01
UpperTria−95	=0.100E−02	Eddy−low	=0.000E+00	Tau,e,t	=0.491E+00
LowerTriang	=0.530E+00	Eddy−up	=0.000E+00	P,add. heati	=0.000E+00
UpperTriang	=0.100E−02	Aturn[eddy]	=0.000E+00	P,ohmic	=0.815E+07
kJb	=0.158E+02	Fz:Halo	=−.544E+03	P,transport	=−.141E+07
kJa	=0.102E+02	Fr:Halo	=0.211E+07	P,alfa	=0.166E+04
Elong−95	=0.166E+01	qionodes	=0.000E+00	P,radiated	=−.908E+05
Elongation	=0.184E+01	FnodeHaloZ	=0.000E+00	Int[p]dv ⋆3/	=0.692E+06
growthtime	=0.000E+00	FnodeHaloR	=0.000E+00	Psb−Ps(Sol)	=0.619E+00
IsLimiter?	=0.000E+00	Ipol@Af0	=−.833E+00	Plasma Ohm P	=0.235E+11
Z[Xpoint]	=−.112E+01	q[halo midp]	=0.231E+02	Peak FW Jt⋆B	=0.000E+00
R[Xpoint]	=0.146E+01	Toroidalflux	=0.183E+02	Z Strike 2	=−.116E+01
Z[Halopoint2	=0.000E+00	Poloidalvolt	=0.000E+00	R Strike 2	=0.110E+01
R[Halopoint2	=0.000E+00	Paramag.tflu	=0.679E−01	Z Strike 1	=−.149E+01
Z[Halopoint1	=0.000E+00	Vloop−low	=0.000E+00	R Strike 1	=0.187E+01
R[Halopoint1	=0.000E+00	Vloop−up	=0.000E+00	Halo:20%peak	=0.100E+01
Z[limiter]	=0.000E+00	(psq−psb)	=0.488E+01	Halo:10%peak	=0.100E+01
R[limiter]	=0.000E+00	(psi)av	=0.759E+01	CEjima	=0.000E+00
Rbar	=0.177E+01	Psi−boundary	=0.462E+01	Res.Flattop	=0.000E+00
rminor	=0.638E+00	Psi−axis	=0.950E+01	Psibar q−saw	=0.000E+00
Rmajor	=0.180E+01	J−axis	=0.323E+07	q−sawteeth	=0.000E+00
Zmax	=0.123E+01	Shear95%	=0.557E+01	Helicity	=0.302E+02
Zmin	=−.112E+01	q95formula	=0.639E+01	Energy:poloi	=0.815E+08
Rmax	=0.244E+01	q95	=0.674E+01	Ext·linked f	=−.192E+01
Rmin	=0.116E+01	qaxis	=0.221E+01	Fz:plasma<>c	=0.173E+05
Zaxis	=0.274E+00	qcyl	=0.520E+01	Lp	=0.307E−05
Raxis	=0.182E+01	Betanormal	=0.146E+00	Fz:PS<>circ.	=0.000E+00
VZjcentre	=0.000E+00	Betastar	=0.138E+00	Fz:PS	=0.000E+00
VRjcentre	=0.000E+00	Betafj	=0.944E−01	Fz:Total−Fz:	=0.144E+07
Zjcentre	=0.246E+00	p−axis	=0.784E+05	Fz:Total	=0.143E+07
Rjcentre	=0.177E+01	betap(1)	=0.113E+00	Circ.|Amp|	=0.230E+08
R⋆Btor	=0.135E+02	li(3)	=0.841E+00	Circ.|Amp|⋆m	=0.173E+09
Time	=0.000E+00	Surface(sec)	=0.215E+01	Power−circ	=0.000E+00
Iplasma	=0.310E+07	Surface(ext)	=0.626E+02	Aturn[circ.]	=0.103E+08

Figure 3. FAST-like Super-X: Snow Flake plasma shape and features.

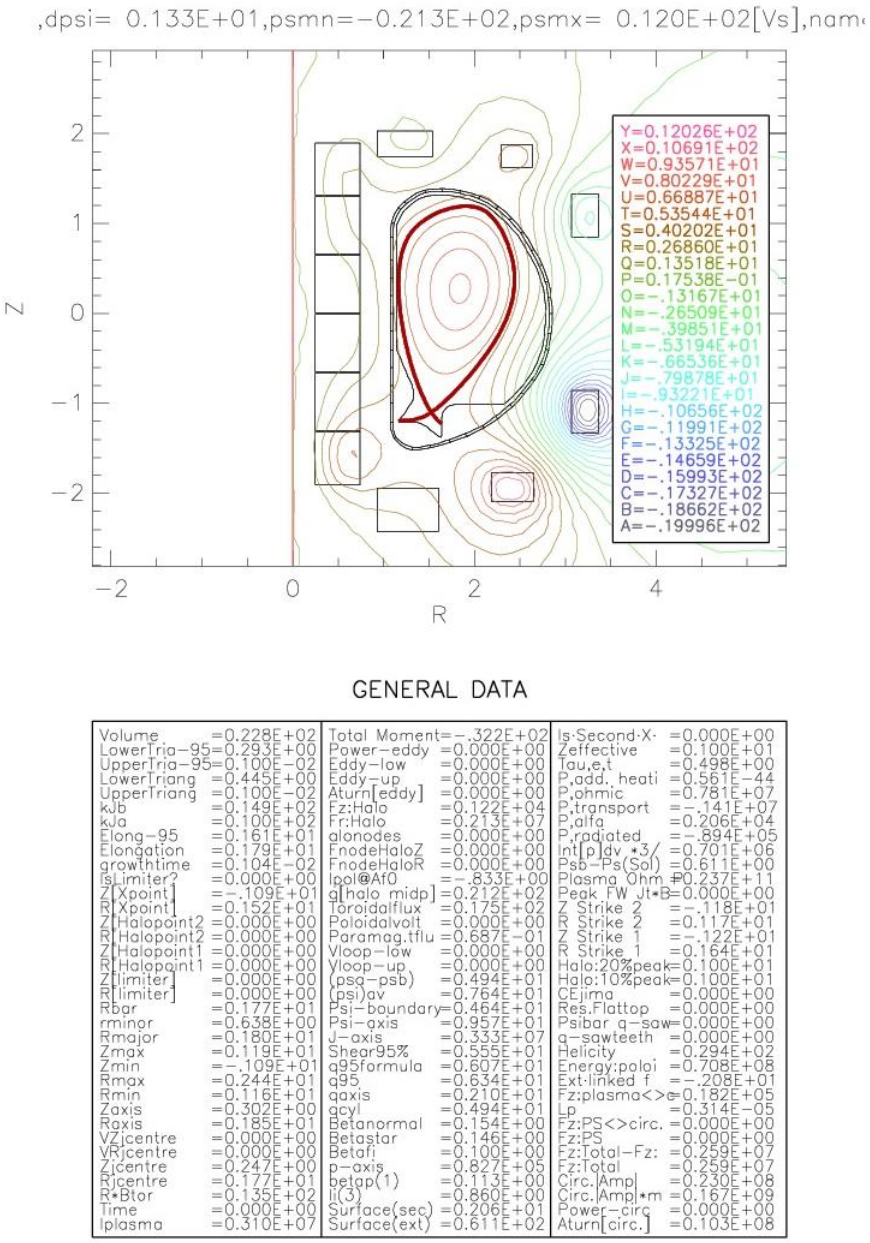

GENERAL DATA

Volume	=0.228E+02	Total Moment	=−.322E+02	Is·Second·X·	=0.000E+00
LowerTria−95	=0.293E+00	Power−eddy	=0.000E+00	Zeffective	=0.100E+01
UpperTria−95	=0.100E−02	Eddy−low	=0.000E+00	Tau,e,t	=0.498E+00
LowerTriang	=0.445E+00	Eddy−up	=0.000E+00	P,add. heati	=0.561E−44
UpperTriang	=0.100E−02	Aturn[eddy]	=0.000E+00	P,ohmic	=0.781E+07
kJb	=0.149E+02	Fz:Halo	=0.122E+04	P,transport	=−.141E+07
kJa	=0.100E+02	Fr:Halo	=0.213E+07	P,alfa	=0.206E+04
Elong−95	=0.161E+01	alonodes	=0.000E+00	P,radiated	=−.894E+05
Elongation	=0.179E+01	FnodeHaloZ	=0.000E+00	Int[p]dv *3/	=0.701E+06
growthtime	=0.104E−02	FnodeHaloR	=0.000E+00	Psb−Ps(Sol)	=0.611E+00
Is,limiter?	=0.000E+00	Ipol@Af0	=−.833E+00	Plasma Ohm P	=0.237E+11
Z[Xpoint]	=−.109E+01	q[halo midp]	=0.212E+02	Peak FW Jt*B	=0.000E+00
R[Xpoint]	=0.152E+01	Toroidalflux	=0.175E+02	Z Strike 2	=−.118E+01
Z[Halopoint2	=0.000E+00	Poloidalvolt	=0.000E+00	R Strike 2	=0.117E+01
R[Halopoint2	=0.000E+00	Paramag.tflu	=0.687E−01	Z Strike 1	=−.122E+01
Z[Halopoint1	=0.000E+00	Vloop−low	=0.000E+00	R Strike 1	=0.164E+01
R[Halopoint1	=0.000E+00	Vloop−up	=0.000E+00	Halo:20%peak	=0.100E+01
Z[limiter]	=0.000E+00	(psq−psb)	=0.494E+01	Halo:10%peak	=0.100E+01
R[limiter]	=0.000E+00	(psi)av	=0.764E+01	CEjima	=0.000E+00
Rbar	=0.177E+01	Psi−boundary	=0.464E+01	Res.Flattop	=0.000E+00
rminor	=0.638E+00	Psi−axis	=0.957E+01	Psibar q−saw	=0.000E+00
Rmajor	=0.180E+01	J−axis	=0.333E+07	q−sawteeth	=0.000E+00
Zmax	=0.119E+01	Shear95%	=0.555E+01	Helicity	=0.294E+02
Zmin	=−.109E+01	q95formula	=0.607E+01	Energy:poloi	=0.708E+08
Rmax	=0.244E+01	q95	=0.634E+01	Ext·linked f	=−.208E+01
Rmin	=0.116E+01	qaxis	=0.210E+01	Fz:plasma<>c	=0.182E+05
Zaxis	=0.302E+00	qcyl	=0.494E+01	Lp	=0.314E−05
Raxis	=0.185E+01	Betanormal	=0.154E+00	Fz:PS<>circ.	=0.000E+00
VZjcentre	=0.000E+00	Betastar	=0.146E+00	Fz:PS	=0.000E+00
VRjcentre	=0.000E+00	Betafi	=0.100E+00	Fz:Total−Fz:	=0.259E+07
Zjcentre	=0.247E+00	p−axis	=0.827E+05	Fz:Total	=0.259E+07
Rjcentre	=0.177E+01	betap(1)	=0.113E+00	Circ.Amp]	=0.230E+08
R*Btor	=0.135E+02	li(3)	=0.860E+00	Circ.Amp]*m	=0.167E+09
Time	=0.000E+00	Surface(sec)	=0.206E+01	Power−circ	=0.000E+00
Iplasma	=0.310E+07	Surface(ext)	=0.611E+02	Aturn[circ.]	=0.103E+08

Figure 4. Current FAST design: Snow Flake plasma shape and features.

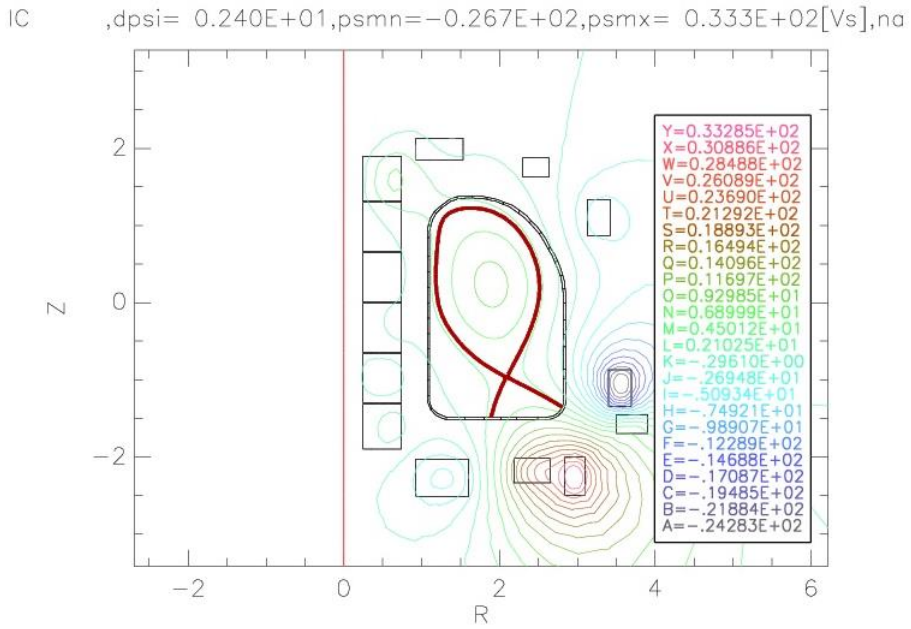

GENERAL DATA

Volume	=0.248E+02	Total Moment	=0.114E+02	Is·Second·X·	=0.000E+00
LowerTria−95	=0.100E−02	Power−eddy	=0.000E+00	Zeffective	=0.100E+01
UpperTria−95	=0.282E+00	Eddy−low	=0.000E+00	Tau,e,t	=0.474E+00
LowerTriang	=0.100E−02	Eddy−up	=0.000E+00	P,add. heati	=0.000E+00
UpperTriang	=0.310E+00	Aturn[eddy]	=0.000E+00	P,ohmic	=0.782E+07
kJb	=0.150E+02	Fz:Halo	=−.171E+04	P,transport	=−.153E+07
kJa	=0.107E+02	Fr:Halo	=0.200E+07	P,alfa	=0.167E+04
Elong−95	=0.154E+01	glonodes	=0.000E+00	P,radiated	=−.951E+05
Elongation	=0.165E+01	FnodeHaloZ	=0.000E+00	Int[p]dv ·3/	=0.725E+06
growthtime	=0.138E+03	FnodeHaloR	=0.000E+00	Psb−Ps(Sol)	=0.608E+00
Is|imiter?	=0.000E+00	Ipol@Af0	=−.833E+00	Plasma Ohm F	=0.241E+11
Z[Xpoint]	=−.961E+00	q[halo midp]	=0.189E+02	Peak FW Jt·B	=0.000E+00
R[Xpoint]	=0.207E+01	Toroidalflux	=0.171E+02	Z Strike 2	=−.149E+01
Z[Halopoint2	=0.000E+00	Poloidalvolt	=0.000E+00	R Strike 2	=0.189E+01
R[Halopoint2	=0.000E+00	Paramag.tflu	=0.669E−01	Z Strike 1	=−.135E+01
Z[Halopoint1	=0.000E+00	Vloop−low	=0.000E+00	R Strike 1	=0.281E+01
R[Halopoint1	=0.000E+00	Vloop−up	=0.000E+00	Halo:20%peak	=0.100E+01
Z[limiter]	=0.000E+00	(psq−psb)	=0.498E+01	Halo:10%peak	=0.100E+01
R[limiter]	=0.000E+00	(psi)av	=0.802E+01	CEjima	=0.000E+00
Rbar	=0.183E+01	Psi−boundary	=0.498E+01	Res.Flattop	=0.000E+00
rminor	=0.666E+00	Psi−axis	=0.996E+01	Psibar q−saw	=0.000E+00
Rmajor	=0.185E+01	J−axis	=0.305E+07	q−sawteeth	=0.000E+00
Zmax	=0.123E+01	Shear95%	=0.377E+01	Helicity	=0.304E+02
Zmin	=−.966E+00	q95formula	=0.612E+01	Energy:poloi	=0.158E+09
Rmax	=0.251E+01	q95	=0.600E+01	Ext·linked f	=−.163E+01
Rmin	=0.118E+01	qaxis	=0.217E+01	Fz:plasma<>c	=0.158E+05
Zaxis	=0.230E+00	qcyl	=0.495E+01	Lp	=0.322E−05
Raxis	=0.188E+01	Betanormal	=0.163E+00	Fz:PS<>circ.	=0.000E+00
VZjcentre	=0.000E+00	Betastar	=0.145E+00	Fz:PS	=0.000E+00
VRjcentre	=0.000E+00	Betafi	=0.100E+00	Fz:Total−Fz:	=0.342E+06
Zjcentre	=0.241E+00	p−axis	=0.775E+05	Fz:Total	=0.340E+06
Rjcentre	=0.183E+01	betap(1)	=0.116E+00	Circ.|Amp|	=0.370E+08
R·Btor	=0.135E+02	li(3)	=0.875E+00	Circ.|Amp|·m	=0.312E+09
Time	=0.000E+00	Surface(sec)	=0.215E+01	Power−circ	=0.000E+00
Iplasma	=0.300E+07	Surface(ext)	=0.638E+02	Aturn[circ.]	=0.905E+07

Figure 5. FAST-like Super-X: Super-X plasma shape and features.

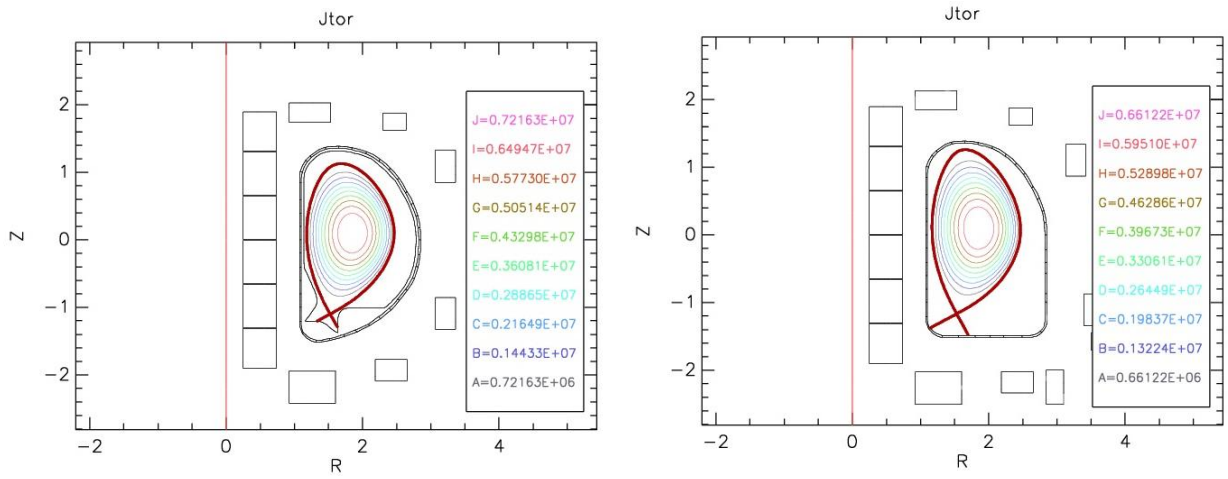

Figure 6. Reference H-mode SN toroidal plasma current density in current (left) and Super-X FAST (right).

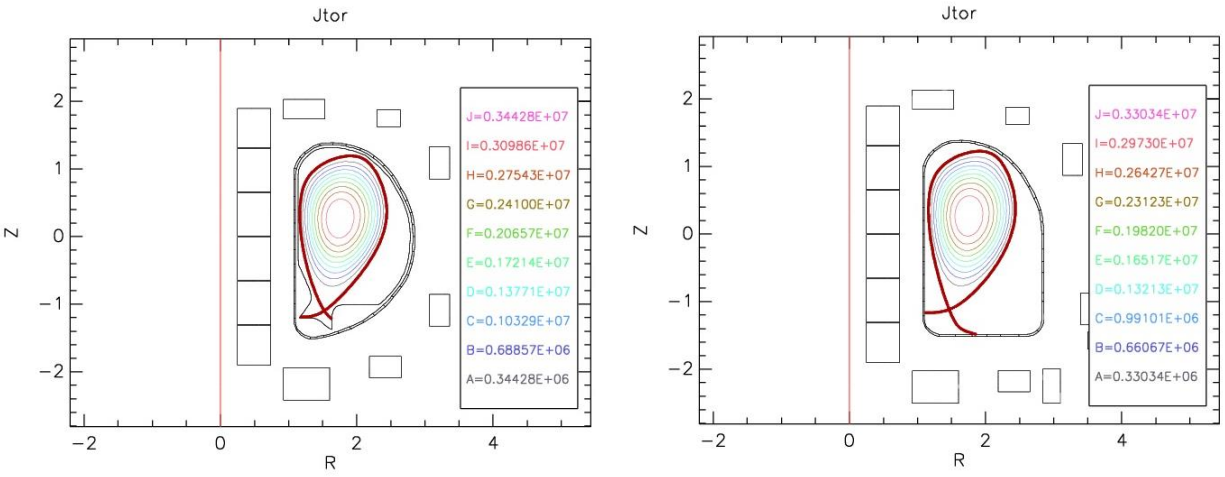

Figure 7. Snow Flake toroidal plasma current density in current (left) and Super-X FAST (right).

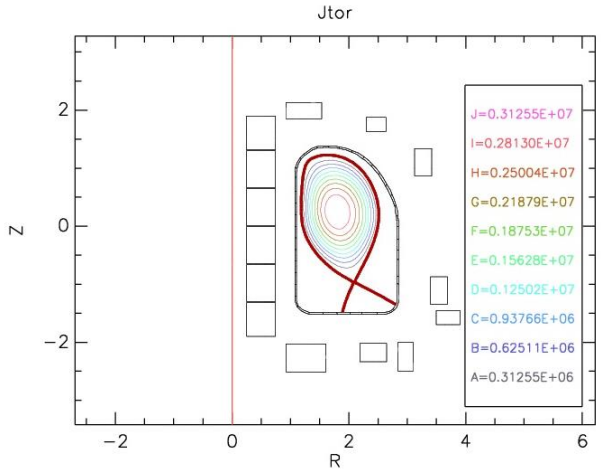

Figure 8. Super-X toroidal plasma current density in Super-X FAST.

The PF coil currents, vertical and hoop Electro-Magnetic (EM) forces in these equilibria are reported for both designs: Fig. 9 (SN), Fig. 10 (SF) and Fig. 11 (SX, only in Super-X FAST). The power supply requirements are not significantly changed when introducing the Super-X capability, except as required by the new PF4a and PF5a coils added. The magnetic poloidal field B due to PF coils and Super-X plasma in Super-X FAST is showed in Fig. 12.

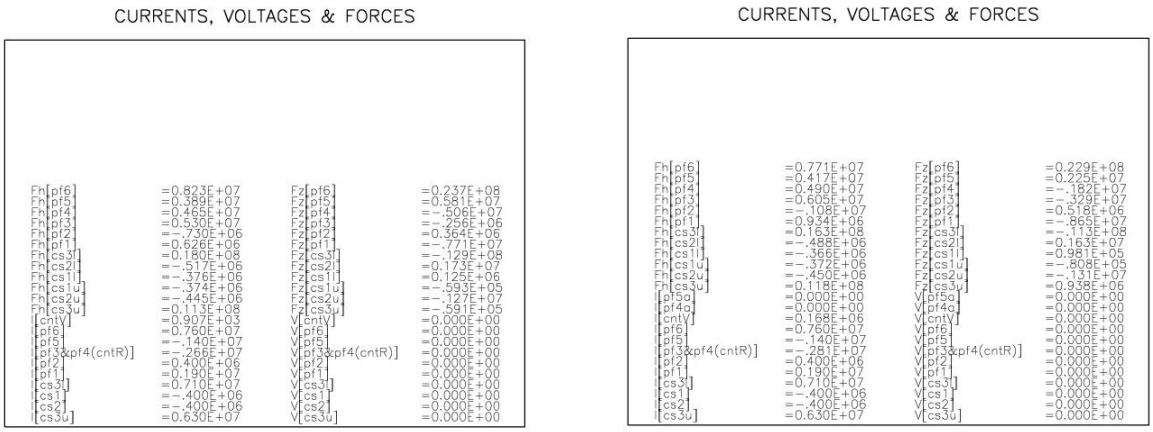

Figure 9. PF currents and EM forces for the H-mode SN equilibrium in current (left) and Super-X FAST (right).

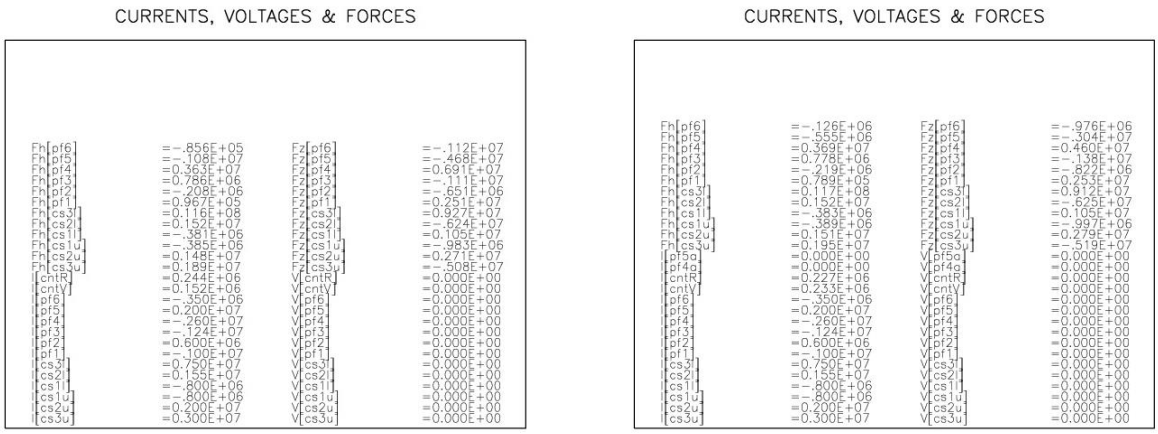

Figure 10. PF currents and EM forces for the Snow Flake equilibrium in current (left) and Super-X FAST (right).

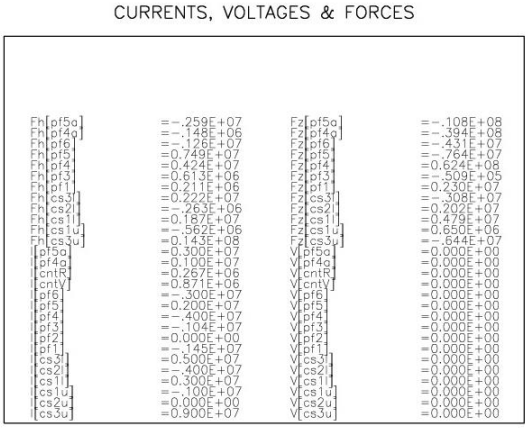

Figure 11. PF currents and EM forces for the Super-X equilibrium in Super-X FAST.

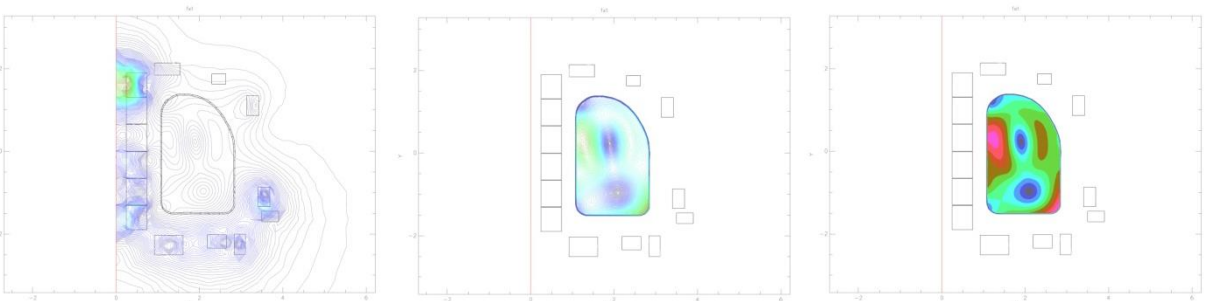

Figure 12. Poloidal magnetic field B due to PF coils and Super-X plasma in Super-X FAST.

2.3 Super-X plasma configuration power exhaust and plasma edge-bulk interaction studies (deliverable D2.3)

To gain insight into the gross effects of geometry alone on the heat flux, we derive a simple analytical expression with the simplifying assumptions that the power which makes it into the upstream SOL follows the field lines to the divertor plate, and we neglect losses from atomic physics. Then the plasma-wetted area A_w on the divertor plates is approximately:

$$A_W = \frac{B_{p,sol}}{B_{div}} A_{sol} \sin(\vartheta) \approx \left| \frac{B_p}{B_t} \right|_{sol} \frac{R_{div} A_{sol}}{R_{sol} B_p / B_t} \sin(\vartheta) = \left| \frac{B_p}{B_t} \right|_{sol} 2\pi R_{div} W_{sol} \sin(\vartheta)$$

where R_{sol}, W_{sol} and A_{sol} are the radius, width and area of the SOL at the midplane, ϑ is the angle between the divertor plate and the total magnetic field B_{div}, and the subscripts p and t denote the poloidal and toroidal directions, respectively. For a plasma with a given W_{sol} and B_p/B_t at midplane SOL, A_w can be increased only by reducing ϑ or by increasing divertor plate major radius R_{div}. Due to engineering constraints, ϑ must be greater than about 1◦, so the only remaining 'knob' to increase A_w is to increase R_{div}. SXD does just this with axisymmetric PF coils. In some cases a large increase in R_{div} can be achieved with relatively small modifications (in positions and currents) to the conventional poloidal field (PF) coils. In Fig. 1 we show two equilibria for a standard aspect ratio (A = 3.5) tokamak (with the poloidal coils within the toroidal one) and a thin tokamak (A = 1.8). with the poloidal coils outside the toroidal one.

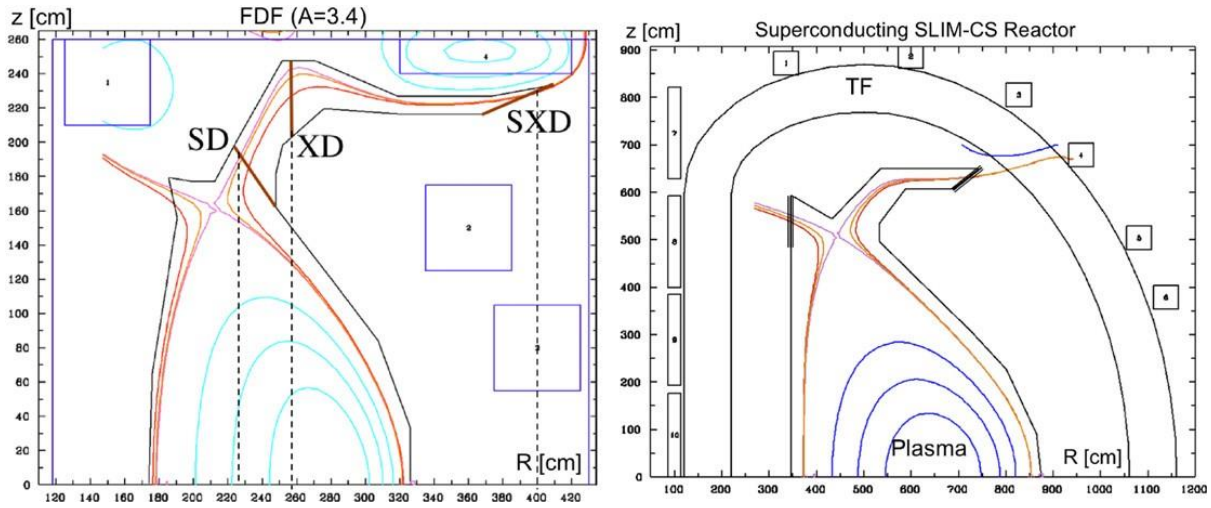

Figure 1. Left: SXD with PF coils inside TF; right: a SLIM-SXD reactor with PF coils outside TF

The simplified semi-analytical models considered here are very helpful in understanding why the temperature can be reduced from very high values to much lower values where additional physical processes, outside these models, can operate strongly.

Simple analytical models shows that the lower value of *total* B field at the divertor plate (due to the larger major radius) can be identified as the dominant causative factor for a reduction in temperature: as a flux tube goes from a region of high B to low B, its cross sectional area increases. Since the power flow through a SOL flux tube is nearly constant (neglecting cross-field transport and atomic effects), the parallel heat flux $Q_{||}$ is reduced as the area is increased. Since the sheath temperature is determined by $Q_{||}$ (but is virtually independent of the plate tilt or poloidal flux expansion), the sheath temperature decreases strongly as the divertor plate is moved towards the lower total B (larger R) region. It is found that this has a much stronger effect on the plasma temperature than the increase in line length. This physical effect is unique to the SXD geometry, since it results from the placement of the divertor plate at much larger major radius and hence lower total B. Other geometries (such as the X-divertor, the snowflake divertor or much stronger plate

tilting) do not have the purely geometrical reduction in the parallel heat flux near the divertor plate that results from the SXD geometry. The simplest divertor model is the 'two-point model' [1], which assumes Spitzer electron heat conduction, pressure balance along a field line and a sheath boundary condition. The effect of B variations can be straightforwardly included, with the assumption that the magnetic field is reduced only near the divertor plate. The results are shown in Fig. 2. For parameters typical of a possible low aspect ratio reactor (CFNS) [2] with an SXD, the reduction in T_{div} is primarily due to reduced B at the plate; the increased line length typical of the SXD is less significant. The SXD gives a low plate temperature for much higher values of the upstream $Q_{||}$ by a factor of about 3.

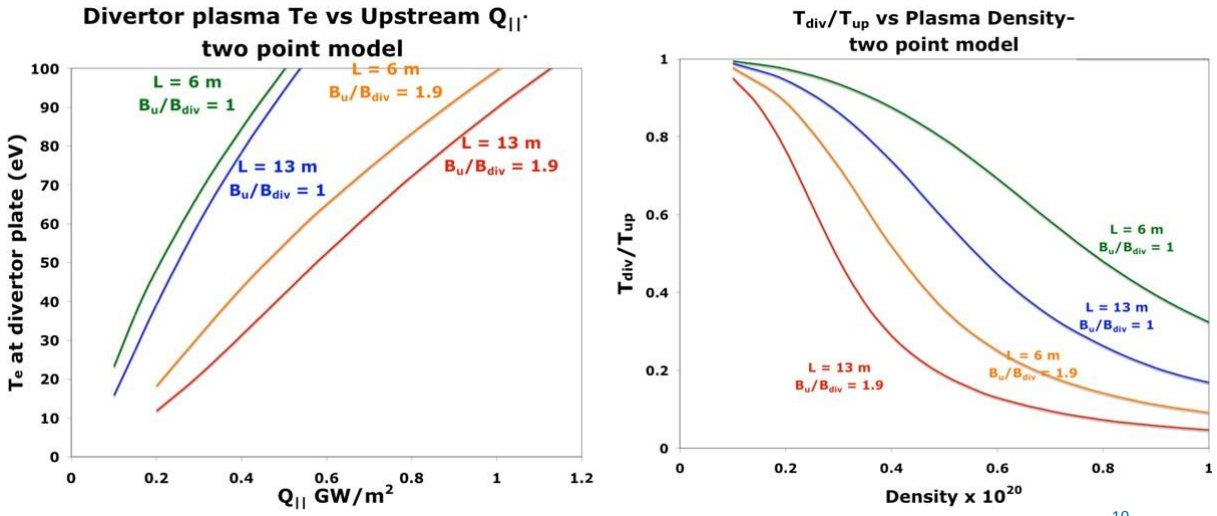

Figure 2. Left: divertor electron temperature versus parallel heat flux for an upstream density of 3×10^{19}; right: ratio of divertor temperature to upstream temperature for a parallel heat flux of 0.5 GWm^{-2}.

3 Conclusions

The cooperation between different people and experience has allowed to deeply analyzing the “Super X” innovative divertor magnetic configuration, underlining both the physics and technological advantages and drawbacks. The Super X configuration, resized on FAST machine like, has clearly show all the technical problems connected when actually proposing it for a machine with an Aspect Ratio $R/a \geq 2$.

4 References

4.1 References for Chapter 2.1

1. F. Najmabadi et al., Fus. Eng. Des., 80 (2006), 3.
2. M. Sato et al., Fus. Eng. Des., 81 (2006), 1277.
3. K. Okano et al., Nucl. Fusion, 40 (2006), 635.
4. C. Gormezano et al., Nucl. Fusion, 47 (2007), S285.
5. M. Kotschenreuther, P. Valanju and S. Mahajan, Phys. Plasmas, 14 (2007), 072502.
6. P. Valanju, M. Kotschenreuther and S. Mahajan, Phys. Plasmas, 16 (2009), 056110.
7. D. Ryutov, Phys. Plasmas, 14 (2007), 06452.

4.2 References for Chapter 2.2

1. P. Barabaschi, The MAXFEA code, (1993), Proc. Plasma Control Technical Meeting, Naka, Japan, April 1993.

4.3 References for Chapter 2.3

1. P. C. Stangeby, The Plasma Boundary of Magnetic Fusion Devices, (2000), Taylor and Francis, London.
2. M. Kotschenreuther et al., Fus. Eng. Des., 84 (2009), 83.

5 Acronyms

3D	three Dimensional
CAD	Computer Aided Design
EM	Electro-Magnetic
FEM	Finite Elements Model
FW	First Wall
MHD	Magneto Hydro Dynamics
PC	Plasma Chamber
PF	Poloidal Field
RH	Remote Handling
SF	Snow Flake
SN	Single Null
SX	Super-X
TF	Toroidal Field
VV	Vacuum Vessel

6 Addendum – CREATE Scientific Expertise

CREATE Consortium (www.create.unina.it) is a no profit research organisation possessing a legal personality; it belongs, according to the Italian law, to the class of Consorzi, where a number of subjects give life to an independent body intended to reach commonly agreed objectives (in the CREATE case, develop, support and stimulate applied research in Electromagnetics).
CREATE was founded in 1992 with the aim of establishing a stable link between industry and university. The partnership is made by the University of Cassino, the University of Napoli Federico II, the Second University of Napoli, the University of Reggio Calabria and the Ansaldo-Ricerche.

CREATE has a very well established experience in the analysis, the design and the operation of tokamak systems, based on the strong interaction between Academy and European Research Centers. In particular CREATE is part of the EURATOM/ENEA Association.
The technical and professional knowledge required for carrying out these activities should cover the three main overlapping areas of the Computational Electromagnetism, Nuclear Fusion Engineering and Mechanical Design. In the following we will summarize the features of the main computational tools available, as implemented and improved on the basis of a very deep experience gained by the CREATE team of scientists in the last twenty years in the electromagnetic analysis of nuclear fusion devices and in the virtual simulation of mechanical systems.
The CREATE team has a very long experience in eddy current calculation, plasma modelling and control design on several experimental devices and specifically on ITER (see [1-34]). The team members were also National Coordinators of various research projects funded by the Italian Ministry of Research about plasma modelling for control. The CREATE team has also a very long experience in CAD modelling and Virtual Reality simulations on complex mechanical assemblies (see [35-74]).
The team has also cooperated with UKAEA on the JET Extreme Shape Controller (XSC) and the upgrade of the JET Control System with particular reference to the vertical stabilization. The team also gave a contribution to the design of ITER from the initial phases of the project, e.g., in "ITER Concept Definition". ITER-1, Oct. 1988, and in ITER DDR e ITER FDR, Final Design Report, 1998. Various team members have been principal investigators of several EFDA contracts on 3D modelling of ITER conducting structures, as well as on the control and the stabilization of ITER plasmas.

CREATE has at its disposal the Virtual Reality Laboratory “VRoom” of the University of Naples Federico II. The lab is mainly devoted to: Computer Aided Design; Virtual Design; Virtual Maintenance, Virtual Manufacturing, Assembly/Disassembly simulations, Virtual Ergonomics, Human Robot Interaction, Virtual Robotics. Active courses provided at undergraduate level are: Virtual Prototyping, Computer Aided Design, Mechanical Drawing, Virtual Ergonomics, Automotive Ergonomics.
The VRoom co-operates with Italian big industries (Alenia Aeronautica, Piaggio Aero Industries, FIAT, Firema Trasporti, Ansdaldo Breda, Ansaldo STS), international Research Centres (VTT in Tampere – Finland, Fraunhofer Institutes - Germany, Supmeca in Paris – France, University of Vigo and Escuela Politecnica de Madrid – Spain, Italian Center for Aerospace Researches - CIRA, ENEA) and many Italian SMEs. The Lab is involved in the Editorial Board of the International Journal on Interactive Design and Manufacturing (IJIDeM) edited by Springer, and in the Scientific Committee of the International IDMME - Virtual Concept Conferences.